OPTICAL INTERFEROMETRY IN FLUID DYNAMICS RESEARCH

by

W. D. Bachalo

and

M. J. Houser

Aerometrics, Inc.

P.O. Box 308

Mountain View, CA 94042

Abstract

Optical interferometry techniques have been applied to the investigation of transonic airfoil flow fields in large scale wind tunnels. Holographic interferometry techniques were used in the study of two-dimensional symmetric NACA 64A010 and supercritical DSMA671 airfoil performance in the NASA Ames 2-by-2-foot Transonic Wind Tunnel. Quantitative data obtained from the interferograms were compared to the surface pressure data. The excellent agreement obtained verified the accuracy of the flow visualization and demonstrated the potential for acquiring quantitative scalar results with interferometry. Measurements of the inviscid flow speed and the boundary layer and wake velocity profiles were extracted from the interferograms and compared to laser Doppler velocimeter measurements. These results were also in good agreement indicating that the flow was sufficiently two-dimensional to obtain reliable (visual), quantitative data from the spatially integrated results provided by the interferometer.

A method for acquiring real-time interferometric data in large scale facilities was developed. This method based on the point diffraction interferometer was successfully tested in the Ames 2-by-2-foot Transonic Wind Tunnel.

The holographic and real-time interferometry methods were applied to the investigations of circulation control airfoils utilizing the Coanda effect. These results revealed the details of the jet interaction with the trailing edge boundary layer and the other parameters affecting the lift augmentation.

Keywords

interferometry, holography, point diffraction interferometry, transonic, supercritical airfoils, circulation control, Coanda effect, laser Doppler velocimeter.

C-3

OPTICAL INTERFEROMETRY IN FLUID DYNAMICS RESEARCH

1.0 Introduction

Optical interferometry has been used as a diagnostic tool in fluid dynamics research for approximately a century beginning with the work of Ernst Mach (1838-1916). More recently, the method has also been used effectively in heat transfer, combustion, and plasma dynamics research. However, the scale of the flow fields that could be addressed with interferometry was severely limited by the coherence of the light source and extreme sensitivity to vibration. These problems were partially alleviated by the development of the laser.

The introduction of holography by Horman [1] and the initial applications to aerodynamic measurements by Heflinger, Wuerker and Brooks [2, 3] represented a notable advance in terms of where the method could be applied. Holographic light wave reconstruction and pulsed lasers provided the means through which the limitations associated with vibration and optical quality were essentially eliminated.

Trolinger [4] applied the method to the visualization of small scale supersonic and hypersonic flow fields. These results suggested the possibility of utilizing the method in large scale

transonic flow field investigations. A holographic interferometer was developed and installed on the NASA Ames 2-by-2-foot transonic wind tunnel for this purpose by the author in 1974. Extensive testing and evaluations of the results were undertaken over the subsequent years. During that time, the method was proven capable of acquiring detailed flow visualization and accurate quantitative data in the NASA Ames 2-by-2-foot, 6-by-6-foot, and 11-foot transonic wind tunnels [5, 6, 7, 8, 9].

Transonic flows proved to be especially suitable to the application of interferometry since compression of the fluid occurs continuously throughout the field, whereas in supersonic flows, the density changes occur primarily through shocks. In addition, the shocks that are present in the transonic flow fields are weak so the entire flow can be assumed to be isentropic. Thus, in the two-dimensional flows studied, the interference fringes were at the same time a mapping of the isopycnics, constant static pressure, flow speed, and Mach contours. These data could readily be reduced with the use of other wind tunnel flow conditions to obtain the quantitative results.

The strong coupling between the inviscid and viscous phenomena in transonic flows predicates the simultaneous observation of the global features of the flow fields and the local viscous-inviscid interactions. Conditions such as the shock boundary layer interaction, turbulence-induced compression waves,

and pressure gradients generated by the model profiles influence the character of the entire flow field. Holographic interferometry furnished the means for obtaining detailed visualization of these flow chracteristics and for producing scalar quantitative data in both the inviscid and viscous regions. By using very short duration exposures, the time-varying phenomena in the flow could be recorded and analyzed. These details are often lost in time-averaged surface pressure and probe measurements.

Several two-dimensional transonic flow fields were investigated using interferometry techniques. The emphasis on helicopter rotor flows led to the investigation of symmetric airfoil flows [5, 6]. These flows posed a significant challenge to the computational fluid dynamicist, and as such, required the acquisition of detailed experimental data. The holographic interferometer and two-component frequency shifted laser Doppler velocimeter (LDV) were combined in an effort to attain these goals. Because of the range of parametric conditions investigated, the interferometry data proved effective in directing the LDV measurements to the regions where flow angle and the turbulence quantities were needed. The detailed flow visualization provided by the interferometer made a significant contribution toward the understanding of the complex fluid dynamics which characterize these flows.

Supercritical airfoils were also studied under a cooperative program with the Douglas Aircraft Corporation and the Ames Research Center [7]. The series of tests were part of an overall program with the goal of completely documenting these flow fields and providing further insights for the improved design of this class of airfoil. Flow fields produced by supercritical airfoils operating at their design Mach number and lift coefficient are characterized by regions of strong viscous-inviscid interactions. These airfoils are also characterized by large aft loading. As such, the iterative procedures used for calculating conventional airfoil flows failed because the initial inviscid calculations were often so different from the actual flow field that convergence to a physically realistic solution did not occur. Simiempirical methods were required for the treatment of the trailing edge region.

The investigations covered under the research program were intended to provide data for comparison with the results of numerical computations. Based on the data obtained in the first phase of the program, modifications were made to the airfoils used in subsequent tests. Laser Doppler velocimeter, surface and pitot pressure data were combined with data from the holographic interferometer to provide an unusually complete description of the flow fields.

Research on advanced rotorcraft utilizing Coanda blowing for circulation control was also supported using holographic interferometry and a new method for real-time interferometry [10]. These investigations were conducted over a period of three years on a number of airfoil configurations operating at transonic speeds. Circulation control airfoils utilizing the Coanda effect introduce an added complexity to the transonic flow fields which increases the difficulty in understanding and predicting these flows. The Coanda effect occurs when a high-velocity jet emits tangentially from a surface slot and remains attached to the surface because of the reduced pressure produced beneath the jet. External fluid is entrained by the jet assisting the flow in remaining attached well-around the typically blunt trailing edge of the airfoil.

Interferometry and other techniques were applied to generate a complete visualization of the flow which helped resolve some of the questions regarding the flow behavior particularly in the neighborhood of the training edge. A range of operating conditions were investigated including the stall condition and jet detachment. Because the understanding of the circulation control airfoil flows at transonic speeds was rather primitive at the initiation of the program, these investigations were needed for elucidating some of the complex phenomena.

In this report, the development efforts that were required in bringing the interferometric techniques to fruition as diagnostics for large scale transonic wind tunnel testing will be reviewed. Comparative measurements are presented to demonstrate the reliability of the flow visualization and quantitative data. Application of a new method for obtaining real-time interferometry data in large scale facilities is also described. The method which is currently under development by Aerometrics has been demonstrated in the Ames 2-by-2-foot Transonic Wind Tunnel.

2.0 Interferometry Techniques

Holographic Interferometer

As a flow diagnostic, the holographic interferometry technique does not differ, in principle, from the Mach-Zehnder method. In comparison, the holographic method creates interference between two reconstructed light waves which have followed similar paths at different times whereas the Mach-Zehnder interferes two light waves from dissimilar paths at the same time. This distinction is important because component imperfections in the optical path tend to cancel when holographic recordings are reconstructed and interfered.

Although there are several ways in which holography can be used as an intermediary for interferometry including double exposure, real-time, and dual plate methods, the latter technique was found to be most useful in aerodynamic applications. With this method, an exposure is made on a holographic (photographic) plate while there is no flow in the wind tunnel. This hologram is later used to reconstruct the reference light wave. Subsequent plates are exposed at the flow conditions under investigation. After processing, the plates are positioned in the reconstruction plate holder, illuminated by a duplicate of the reference beam, and aligned for the infinite fringe mode. One reference plate can be used consecutively with plates taken at the test conditions. Vibrations in the system are insignificant because the exposure duration is extremely short (20 nanoseconds). Random displacements between images on the plates are accounted for in the reconstruction process.

One major difficulty arises when utilizing the dual plate technique. If the density of the flow is disturbed over the entire field of view, as is often the case, it is difficult to ascertain when the interferometer is aligned to the infinite fringe condition. That is, to the case wherein fringes only occur as a result of changes in the flow density. Fortunately, a knowledge of the transonic flow characteristics and other alignment criteria have led to accurate reconstructions that produced results in good agreement with other measurements.

The first conversion of the wind tunnel schlieren system to holography utilized a pulsed ruby laser with a helium neon laser for alignment. Ruby lasers produce sufficiently high energy (50 millijoules) pulses of short duration (20 nanoseconds) to "freeze" the flow being recorded. These lasers also have a coherence length on the order of one meter which simplified the alignment requirements. Holograms produced with the ruby laser had good diffraction efficiency but the alignment of the system tended to be very time consuming. This was due primarily to the relatively long time periods (30-60 seconds) required between laser firing and the need to align with a separate CW laser. Optical path lengths on the order of 30 meters and the makeshift optical system supports exacerbated the problem.

Based on the feasibility investigations using the ruby laser and a makeshift optics system, a permanent instrument was designed and installed in the Ames 2-by-2-foot facility. A Quanta Ray DCR-1 Nd:YAG laser was used as the light source. The Nd:YAG laser is capable of producing pulse repetition rates between 1/sec and 22/sec at up to 80 mJ of energy in the frequency doubled green line (0.532 m). The Quanta Ray DCR-1 laser produces a beam that has a so-called "donut" intensity distribution due to the laser cavity's unstable resonator configuration. Thus, a means was required to transform this intensity profile into a filled-in beam with a quasi-gaussian shape.

The optical system consisting of a transmitter and receiver stage is shown in Figure 1. In order to transform the beam intensity profile, a combination of a lens and spatial filter with a 150 micrometer aperture was used. The beam was then split into two paths with a beamsplitter. The object or information beam was reflected from the beamsplitter and expanded to overfill the schlieren mirror. With the foci of the expansion lens and schlieren mirror coinciding, a collimated beam was formed and transmitted through the wind tunnel test section. The object beam which was 46 cm in diameter was received by a second spherical schlieren mirror and refocused to the receiver stage. An additional lens was used to collimate the beam at an appropriate size for recording at the holographic plate holder.

Laser light transmitted through the beamsplitter was passed under the wind tunnel via a trench. Because of the long optical paths, a beam collimating system was provided to control the beam divergence. Optical path length matching was achieved with mirrors used to fold the beam within the trench. The reference beam was expanded and collimated to 90 mm in diameter at the receiver and directed onto the holographic plate.

The angle of intersection of the object and reference beams at the holographic plate was kept small enough to produce interference fringes that were within the spatial frequency resolution of the film. Beam intersection angle determines the

spatial carrier frequency which has variations due to the flow field superimposed on it. Thus, an adequate margin on the frequency is required to ensure adequate diffraction efficiency of the holograms.

Point Diffraction Interferometer

A relatively new interferometry concept was investigated for feasibility in compressible flow applications. The method was attractive in that it presented the possibility of providing real-time interferometric results.

The point diffraction interferometer (PDI) as described by Smartt [11] is like some other forms of radial shear interferometers insofar as it has the unique configuration wherein the light is divided into two components to produce the test and reference waves, after passing through the test field. However, the PDI is the only known concept capable of producing the quantitative information on the light wave distortion directly.

With the PDI, the spherical reference wave is generated by diffraction at a point discontinuity located in the path of the beam. The discontinuity can be either a circular aperture or an opaque disk. Figure 2 illustrates the principle of operation. The aperture (or opaque disk) is located at the image of the wavefront to be analyzed. In the embodiment proposed by Smartt, an aperture in an absorbing film or an otherwise nondiffracting

substrate was used. Light incident upon the film and aperture is transmitted with a reduction in amplitude while the aperture produces a spherical diffracted wave. If the aperture is sufficiently small, a spherical diffracted wave is produced which will then interfere with the entire transmitted test wave.

Movement of the aperture along the optical axis away from the focal plane will produce circular fringes. Lateral movement of the aperture can be used to produce linear fringes for finite fringe operation. Deliberate displacement of the aperture will reduce the intensity of the diffracted wave which, in turn, reduces the visibility of the resulting fringes.

The important parameters effecting the visibility of the resulting fringes are the aperture size and the relative film and aperture transmittances. The cone angle defined by the first minimum in the diffraction pattern should be greater than that of the receiver system. These requirements can be satisfied with the proper selection of the aperture size. However, in the special case of fluid dynamics applications, where the wave distortions are expected to be large, the fulfillment of these requirements will become more difficult.

Another requirement that is specific to fluid dynamics applications is the need for very short duration exposures to freeze the motions in the flow field. Short exposures, in turn, demand the use of high power continuous wave (CW) or pulse

lasers. The use of substrates with apertures or disks cannot withstand such high energy levels. Our preliminary tests demonstrated that, even at very low energy levels, the pulsed laser burned holes in the substrates rendering the device inoperable.

Because of the large range of wave distortions present in fluid dynamics applications, a greater range of amplitudes in the diffracted and transmitted waves will occur. The distribution of energy incident upon the aperture will be significantly reduced when the focused beam is spread as a result of the flow field turbulence and refractive gradients in the inviscid flow. With relatively weak disturbances to the wavefronts, a greater amount of energy will be focused onto the aperture resulting in a greater amplitude in the diffracted wave. The resulting changes in the amplitudes of the focused beam will produce large variations in the relative intensities of the object and reference waves which will reduce the visibility of the interference fringe pattern, possibly to an extent where the pattern may be imperceptible. Some of these difficulties can be corrected by changes in the size of the aperture and the relative absorption of the substrate. However, if the aperture is too large, the diffracted cone of light will be too narrow and some of the distorted wave could appear on the diffracted wave. By increasing the absorption of

the substrate the possibility of burning it out is increased and there may be insufficient energy for the high speed recordings.

Clearly, the advantages of the technique which include relative simplicity of operation, insensitivity to vibration, and the opportunity for real-time recording suggested that attempts to modify the concept were worthy of attention. The aforementioned limitations to the application of the method in fluid dynamics research could be solved by redesigning the optical configuration.

A great deal of flexibility in the operation of the method was achieved with the optical configuration shown in Figure 3. A similar concept was also considered by Howes [13]. The layout of the system was the same as for a schlieren system up to the receiver section. Either a CW or pulse laser could be used as the light source. Because the path lengths can be carefully matched, in principle, a white light source could also be used. The light beam must be spatially filtered and expanded to fill the lenses or mirrors of the transmitter system to form a collimated beam. The field to be tested is located in the beam path, as with a conventional schlieren system. The receiver mirror serves to focus the light after passing through the test section. At the receiver, the beam was split into two optical paths with a beamsplitter. The transmitted beam was spatially filtered to remove the high spatial frequencies which were produced by the refractive field in the test section. This diffracted beam forms

the reference wave. The reflected beam retains the wave distortion information produced by the refractive field. It was then recombined with the reference wave. This section of the system was aligned in the same manner as a common Mach-Zehnder interferometer. However, optical components on the receiver section were made very compact and were rigidly mounted such that vibration was no more serious than for a schlieren system.

Inasmuch as this configuration complicates the technique, it also offered the needed flexibility for the application of the method in fluid dynamics investigations. First of all, the use of two separate optical paths allowed the reduction of energy incident upon the aperture. The apertures could now consist of pinholes that would withstand the high energy levels and which were commerically available. Because of the losses involved in the filtering process, a variable beamsplitter was used instead of an absorbing substrate to maximize the use of the available light. Additional attenuation may be introduced to maximize the visibility of the interference fringe pattern and, hence, the signal-to-noise ratio. Both the transmitted and reflected images produced by the beamsplitter may be exploited. One image can be used for real-time viewing while the other is being recorded.

The description of the amplitude and angular distribution of light scattered by a circular aperture used in the interferometer can be approximated by the Fraunhofer diffraction theory as

$$I_{sca}(\Theta, d) = I_0\left(\frac{\pi d^2}{4\lambda}\right)^2\left[\frac{J_1\left(\frac{\pi d}{\lambda}\sin\Theta\right)}{\left(\frac{\pi d}{\lambda}\sin\Theta\right)}\right]^2$$

where Θ is the scattering angle measured from the incident beam, I_o is the incident beam intensity at the aperture, d is the aperture damager, λ is the laser wavelength, and J_1 is the first order Bessel's function of the first kind. Using this expression, the diffraction pattern can be matched to the numerical aperture of the collimating lens of Figure 3. Estimates of the relative intensities of the reference and object wave were also made.

The method was tested in the laboratory by introducing phase shifts in the beam, optically filtering it and then interfering the filtered wave with a test wave that was spherical or planar as appropriate. With this procedure, the filtering was evaluated under controlled levels of distortion on the incident waves. The relative transmission efficiency was measured. Several combinations of transform lenses and apertures were considered in the analysis. The controlling parameter was the intensity incident upon the pinhole. A short focal length lens would increase the intensity but would accelerate the burnout of the pinhole. On the other hand, a long focal length lens and larger pinhole would require a much longer focal length lens to collimate

the filtered reference beam at a diameter large enough to overlap the object or data beam.

These considerations also affected the selection of the recording media. In the early stages of the investigation, polaroid, 4" X 5" sheet, 16mm movie, and 35mm film was used. Estimates of the film resolution were made based upon the previous work with holographic interferometry. For example, the fringe spacing in the boundary layer of a supercritical airfoil was approximately 0.5mm. If the entire field of view was recorded (450mm), the approximate resolution for 4" X 5" film would be 10 lines per mm. On 35mm film, this represents a spatial resolution of approximately 30 lines per mm. Using 16 mm movie film, the resolution must be approximately 60 lines per mm. This is at the resolution limit of conventional films. High speed film generally has large grain size and lower resolution.

Thus, it was important to maximize the intensity on the pinhole in order to relax the requirements on the recording media. In an effort to mitigate this requirement, it was instructive to recognize that the scattered intensity (intensity of the reference) beam increases as the square of the aperture diameter. It is also known from diffraction theory that the angular distribution of the scattered light decreases as 1/d (eg. $\omega \approx \frac{1.22\pi R}{d}$). If the aperture diameter and distance to the point of observation was increased by a factor of two, the area of

the reference beam would remain essentially the same. However, the intensity was increased by a factor of 4. The aperture size is limited by the relative distortion on the incident beam. If the aperture is too large relative to the focused incident beam, the diffracted wave will carry a distorted component of the incident wave.

Further parametric studies of the optical filtering are being carried out in the continuation of the research program. Optimization of the filtering aperture requires considerations that include pinhole survival, spatial filtering, reference beam intensity, and susceptibility to misalignment.

Data Reduction

Obtaining quantitative results from the interferograms is straightfoward for two-dimensional flows. The pathlength through the wind tunnel in the present case was 61 cm so the density changes at the test flow Mach numbers was sufficient to produce an optimum number of interference fringes in the infinite fringe mode. Using the infinite fringe mode has the advantage that the fringes produce a direct mapping of the constant density contours.

Evaluation of the density change per fringe can be determined using the following relationships. In an inhomogeneous density test field the phase shift of the light wave is

$$\left(\frac{\Delta\phi}{2\pi}\right) = \frac{1}{\lambda} \int_{\zeta}^{\zeta_1} [n(x,y) - n_o]dz$$

where is the laser wavelength and n is the index of refraction. When the interferometer is aligned in the infinite fringe mode, the equation of the fringes is

$$\int_{\zeta}^{\zeta_1} [n(x,y) - n_o]dz = N\lambda$$

where N is an integer. Applying the Gladstone-Dale Constant relating phase variation to density, the integrated relationship is

$$\rho(x,y) = \rho_o + \frac{N\lambda}{KL}$$

The constant values used in the tests to be described were:

$$L = 609.6 \text{ mm}$$

$$= 0.532 \text{ m}$$

$$K = 0.226 \text{ (gm/cm}^3)^{-1}$$

$$\frac{\lambda}{KL} = \frac{0.532 \times 10^{-3} \text{ mm}}{0.226 \text{ (gm/cm}^3)^{-1} \; 609.6 \text{ mm}}$$

Combining the constants and adjusting for the wall boundary layers result in:

$$\rho_1 - \rho_0 = 2.46 \times 10^{-4} \frac{\text{lbm/ft}^3}{\text{fringe}}$$

It remained to identify a particular fringe to be used as the reference with its corresponding density. This was done in several ways. If there was a region of undisturbed flow in the field of view, the wind-tunnel conditions could be used. Unfortunately, this was not generally the case. Instead, a surface pressure measurement was converted to density by using the total temperature, T_o, and the total pressure, P_o. Another independent reference could be obtained from the inviscid flow velocity measured with the laser velocimeter, for example.

Flow Fields Investigated

The experiments which produced the examples in this paper were conducted in the Ames 2-by-2-foot Transonic Wind Tunnel. This tunnel is a closed-return, variable density flow facility with 21% open porous-slotted upper and lower walls for transonic testing. The airfoils tested were a NACA 64A010, a Douglas Aircraft Corporation DSMA671 supercritical airfoil and several circulation control airfoils utilizing the Coanda effect. Wind tunnel test conditions ranged from a free-stream Mach number of

0.3 to 0.9 and chord Reynolds number of 10^6 to 2 x 10^6. Transition strips were used on the upper and lower surfaces of the airfoils to ensure fully developed turbulent flows.

3.0 Results and Discussions

Interferometry data were obtained over a range of conditions and the quantitive results compared to measurements obtained by other means. Because of the possible uncertainties in the alignment of the reconstructed light waves, a series of tests were deemed necessary to determine how accurately the waves could be aligned to the infinite fringe mode.

Evaluation of the optical system was conducted using pairs of holograms exposed with no flow in the wind tunnel. Reconstruction of the two light waves and alignment of the waves to the infinite fringe mode ideally should result in no fringes over the field of view. Typically, one or two fringes would occur after careful alignment. This was considered to be an acceptable level of error considering the number of fringes present under the test conditions.

Interferograms could not be trusted even for flow visualization in the initial phase of the instrumentation development. With the light wave over the entire field of view disturbed due to the flow, Figure 4, the alignment of the

interferometer was uncertain. Thus, the interferometric results were reduced to basic flow parameters and compared to measurements with other means. The most readily available and reliable data is the surface pressure distribution.

With the assumption of isentropic flow, the densities measured from the interferograms were reduced to surface pressure coefficient by the relationship

$$C_p = \frac{2}{\gamma M_\infty^2}\left[\left(\frac{P}{P_t}\right)\left(\frac{P_t}{P_\infty}\right) - 1\right]$$

and

$$\frac{P}{P_t} = \left(\frac{\rho}{\rho_t}\right)^\gamma$$

where M_∞ is the freestream Mach number, $\gamma = 1.4$, and P_t and ρ_t are the pressure and density at the stagnation conditions. The density of one of the fringes was identified using a pressure measurement at one point in the flow. Fringes were then simply counted from the reference to obtain the density at each point in the flow field.

Agreement between the measured surface pressure and the interferometric data, Figure 5 was generally very good which confirmed the interferometric results. It should be recognized

corrected downstream total pressure offered only a slight improvement in the pressure distribution.

Experiments were also conducted on supercritical airfoils for the Douglas Aircraft Corporation [7], Figure 8. Supercritical airfoils characteristically have flat upper surfaces to maintain shock-free flow or to hold the shock well aft on the airfoil. The trailing edge had a lower surface concavity which produced a relatively large aft loading. Comparisons to the 64A010 airfoil showed that the closed fringe contours in the primary inviscid flow were symmetrically located above and below the trailing edge. By contrast, the closed contours were displaced streamwise in the interferograms corresponding to the supercritical airfoils, indicating local maxima of pressure both in the lower-surface concavity and downstream of the trailing edge on the upper surface of the near wake.

The interferogram data provided static pressure distributions at the outer edges of the boundary layer and near wake, Figure 9, which are difficult to measure by other techniques. Significant static pressure gradients normal to the streamlines could be present in the near wake flows produced by supercritical airfoils. Pressure variations also occurred across the lower-surface boundary layer in the lower surface concavity. These data were used to correct the boundary layer and wake profile measurements using pitot and static pressure probe measurements.

that the surface pressure data represents time-averaged results obtained at points on the midspan of the airfoil. The interferometric results were spatially averaged over the span of the airfoil but recorded at an instant in time. Thus, the good agreement in the results also confirmed the relative two-dimensionality of the flow. A small difference in the data have occurred in the neighborhood of the shock. This was due to the interaction of the shock with the sidewall boundary layers. The interaction typically causes the shock to move forward at the sidewalls.

At an airfoil angle of attack of 3.5^{o} wherein the shock was relatively strong, there was a concern with the loss of total pressure across the shock producing errors in the data. However, the good agreement with the pressure data verified that the total pressure loss across the shock and, hence, the change in entropy, was insignificant. With an increased angle of attack to 6.2^{o}, Figure 6, massive shock-induced separation occurred. There was uncertainty as to whether the interferometric data obtained at the outer edge of the separated boundary layer would provide an accurate representation of the surface pressure in such cases. However, the results shown in Figure 7 demonstrated the very good agreement achieved even with a strong shock and severe flow separation. An estimation of the shock strength was made to obtain an estimation of the loss in total pressure. Using the

Once the relative accuracy of the interferometry data was confirmed, the Mach contours determined from

$$\frac{\rho}{\rho_t} = \left(1 + \frac{\gamma-1}{2} M^2\right)^{-\frac{1}{\gamma-1}}$$

were traced from the interferograms. The Mach contours provide a quantitative mapping of the global features of the flow and are valuable for comparisons to numerical predictions of the inviscid flow field.

The flow speed was determined from the density distribution using the assumption of isentropic flow of a perfect gas and the relationship

$$\frac{V}{C_t} = \left[\frac{2}{\gamma-1}\left(1 - \left(\frac{\rho}{\rho_t}\right)^{\gamma-1}\right)\right]^{\frac{1}{2}}$$

where c_t is the speed of sound at the stagnation or total conditions. Figure 10 shows the flow speed data compared to laser Doppler velocimeter measurements. The results were in very good agreement indicating that flow speed measurements could be easily obtained for the inviscid flow. This represents an efficient

means for mapping the flow speed when coupled with the laser Doppler velocimeter to obtain flow angle information where this parameter cannot be inferred from the model geometry.

Viscous flow information may also be obtained from the interferograms. One of the advantages of the interferometry method when applied to aerodynamics investigations is the ability to visualize the boundary layer and wake flows. This information can be used to direct the laser Doppler velocimeter or other probe methods to regions of interest in the flow. In addition to the flow visualization, flow speed within the viscous layer may also be obtained. Assuming constant pressure across the layer, Crocco's relationship given by

$$\frac{T}{T_e} = 1 + r\,\frac{\gamma-1}{2}\,M_e^2\left[1 - \left(\frac{U}{U_e}\right)^2\right] + \frac{T_w - T_{ad}}{T_e}\left(1 - \frac{U}{U_e}\right)$$

and the perfect gas law. T_e, T_{ad}, and T_w are the edge, adiabatic, and wall temperatures, and r is the turbulent recovery factor which is set equal to 0.88.

Comparisons were made to boundary layer and wake profiles measured with pitot probes and the laser Doppler velocimeter. Representative results obtained on the supercritical airfoil, Figure 8, are presented in Figure 11. Overall, the measurements

were in good agreement. However, the differences in the minimum flow speed regions may have been due to slight three-dimensionality in the wake and to the reduced sensitivity of the interferometer in this region. At low flow speeds, the density change is very small with variation in velocity.

A program of testing was performed to evaluate circulation control airfoils utilizing the Coanda effect. Circulation control airfoils produce a rather complex flow field that is associated with the high speed jet interacting with the turbulent boundary layer. Although the entire flow field was of interest, attention was focused on the jet flow entrainment mechanisms at the trailing edge. This region of flow does not lend itself to measurements by probes or the laser Doppler velocimeter because of the small scales involved and the proximity to a reflecting surface.

Holographic interferometry data were obtained over a wide range of parameters including Mach numbers, Reynolds numbers, angles of attack, and Coanda blowing pressures [13]. Because of the very large lift coefficients produced and the interaction of the Coanda jet with the sidewall boundary layers, there was justifiable concern with three-dimensionality in the flow. As in the previously described investigations, comparisons of the interferometric data to surface pressure measurements were used to evaluate the results. The results were found to be in very good agreement except over the Coanda jet. In this region, there was a

substantial normal pressure gradient between the inner and outer parts of the jet. Thus, the differences were expected and acutally provided a means for determining the normal pressure gradient.

In the absence of blowing, the boundary layers separated from the airfoils at approximately the tangency points where the change in body curvature began for the blunt trailing edge. With Coanda blowing the flow remained attached much further around the trailing edge. This movement of the rear stagnation point produced increased circulation. Circulation typically increases with increased blowing until stall occurs. One type of stall that occurred was a result of jet detachment which was documented in this work.

The degree of jet mixing that takes place determines the ability of the jet to entrain the external flow. How effective this entrainment process is, depends upon the character of the incident turbulent boundary layer. Upstream shock strength, compression waves and the trailing edge pressure gradient produced by the airfoil geometry will thus influence the efficiency of the Coanda jet. These pheomena were effectively visualized using the interferometry techniques and quantitative results were correlated with the airfoil performance. Only the preliminary results of these investigations can be presented since the remaining data

have been classified because of their importance to the DARPA X-Wing Program.

Figure 12 is a typical example of the flow fields studied. The airfoils are typically elliptic in shape with or without camber. With blowing, the flows revealed a very high streamwise pressure gradient at the trailing edge as indicated by the close spacing of the fringes in that area. The local pressure maxima represented by the center of the concentric fringe patterns moved upstream to the trailing edge of the airfoil as the blowing was increased. The rear stagnation point became localized and was observed to move around the trailing edge.

Interferometry provided a very efficient means for visualizing the details of the flow at the trailing edge of the airfoil. Figures 13 a and b show typical results for the unblown (13a) and the blown (13b) cases. The fringes running essentially parallel to the flow represent the boundary layer and the small notch on the upper surface is the blowing slot (h=250 micrometers). Without blowing, the boundary layers separated from the airfoil and produced a large wake. When blowing was introduced, the boundary layer became entrained by the jet. The jet is clearly visible around the trailing edge. The ability to visualize these features of the flow and obtain incident boundary layer data is valuable to the aerodynamicists and the

computational fluid dynamacists attempting to predict these flow fields.

The real-time point diffraction interferometry method was also used in this series of tests. However, before implementing the method in the wind tunnel, several laboratory tests were conducted to ensure that the results produced were reliable. Comparisons of interferograms obtained using holography were made for simple free convection flows (Figure 14). The results were essentially identical. One significant advantage of the real-time interferometer was the speed with which the results could be obtained. Using Polaroid film, the real-time interferogram was available in a matter of seconds whereas the holographic interferometer required approximately 20 minutes.

A makeshift optical system for the PDI method was installed on the Ames 2-by-2-foot transonic tunnel. Both the Nd:YAG laser and an 18-watt Argon-ion CW laser were alternately used as the light source. A high speed movie camera was used to record the interferometric data. No special vibration isolation equipment was required even in the wind tunnel environment.

Real-time viewing of the interferometry results proved to be an excellent means for visualizing the flow field phenomena. Dynamic events such as the vortex shedding and the turbulent interactions of the Coanda jet and the boundary layer are often lost when recorded on single exposures. Relative motion between

the various parts of the flow provided the added dimension needed to better understand the flow behavior. Although not recognized in the still images, large scale aperiodic shedding of vorticity was clearly visible at certain flow conditions. Recordings of these flow phenomena were made on movie film at 400 frames per second. This framing rate and shutter speed were adequate in preventing the blurring of the fringe patterns as a result of flow field unsteadiness.

Unfortunately, these results have been classified as proprietary by NASA and, thus, were not available for this report.

4.0 Summary and Conclusions

Although holographic interferometry was previously used for flow field visualization and to obtain some quantitative results in small wind tunnels (13 cm X 13 cm), it had not been utilized in full scale facilities. The program of research on transonic flow fields conducted at the NASA Ames Research Center was successful in demonstrating the potential of the interferometry techniques. Because the interferometry data from the two-dimensional flows was easy to interpret and reduce to quantitative results, the reliability and accuracy of the method were easily confirmed by comparison to measurements by other means. The method provided detailed flow visualization of the entire flow

field and produced accurate results for both the inviscid and viscous flow.

A new interferometry method was developed and applied to flow field investigations. The method promises to provide a valuable alternative to holographic interferometry for practical aerodynamics research. Real-time interferometric results made available with the method enhanced the level of detail available to the experimental fluid dynamicist.

Future development efforts are planned for improving the point diffraction interferometer (PDI) system. The availability of real-time interferometry and the very high data recording rates that can be achieved places added importance on data reduction techniques. Aerometrics personnel are currently investigating methods for reducing the interferometry results from the PDI on-line. Methods have been considered that can produce the quantitative results in essentially real time.

5.0 Acknowledgements

This work was supported by the NASA Ames Research Center, Aerodynamics Branch and the X-Wing Project Office. Work on the supercritical airfoils was supported in part, by the Douglas Aircraft Corp.

6.0 References

1. M. H. Horman, "An Application of Wavefront Reconstruction to Interferometry," Appl. Opt. 4, 333-336 (1965).

2. R. E. Brooks, L. O. Heflinger, and R. F. Wuerker, "Interferometry With a Holographically Reconstructed omparison Beam," Appl. Phys. Letters, 7, 248-249 (1965).

3. L. O. Heflinger, R. F. Wuerker, and R. E. Brooks, "Holographic Interferometry," J. Appl. Phys., 37, 642-649 (1966).

4. J. D. Trolinger, "Laser Instrumentation for Flow Field Diagnostics," AGARD-AG-186, 1974.

5. W. D. Bachalo, and D. A. Johnson, "Laser Velocimetry and Holographic Interferometry Measurements in Transonic FLows," Laser Velocimetry and Particle Sizing," Hemisphere Publishing Corp., 1979, edited by H. Doyle Thompson and Warren H. Stevenson.

6. D. A. Johnson, and W. D. Bachalo, "Transonic Flow Past a Symmetrical Airfoil-Inviscid and Turbulent Flow Properties," AIAA Journal, 78-117R, Vol. 18, No. 1, January 1980, p. 16.

7. F. W. Spaid, and W. D. Bachalo, "Experiments on the Flow About a Supercritical Airfoil Including Holographic Interferometry," Journal of Aircraft, Vol. 18, No. 4, April 1981.

8. W. D. Bachalo, "An Experimental Investigation of Supercritical and Circulation Control Airfoils at Transonic Speeds Using Holographic Interferometry," AIAA Paper No. 83-1793, Danvers, Massachuetts, July 1983.

9. W. D. Bachalo, "An Experimental Investigation of Circulation Control Flow Fields Using Holographic Interferometry," NASA Contract Report CR 166482, 1982.

10. W. D. Bachalo and M. J. Houser, "A Real-Time Interformeter Technique for Compressible Flow Research," Paper No. 84-1600, AIAA 17th Fluid Dynamics, Plasma Dynamics and Laser Conference, Snowmass, Colorado, June 1984.

11. R. N. Smartt, "Special Applications of the Point-Diffraction Interferometer," SPIE, Vol. 192, Interferometry, 1979.

12. Walton L. Howes, "Large-aperture Interferometer with Local Reference Beam," Applied Optics, Vol. 23, No. 10, May 1984, p. 1467.

13. W. D. Bachalo, "Investigations of Circulation Control Airfoil Flow Fields at Transonic Speeds," NASA Contract Report 1983.

LIST OF FIGURES

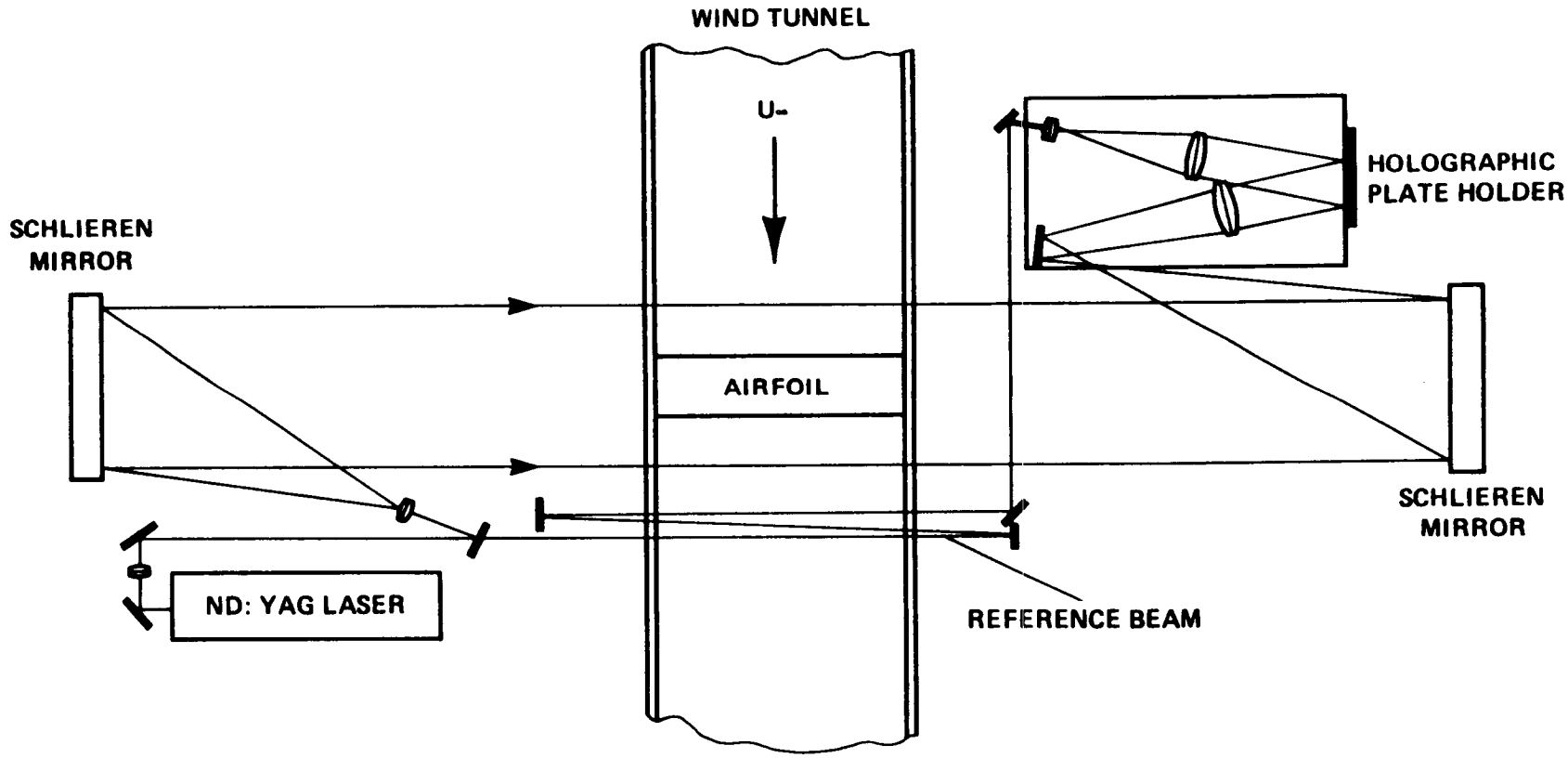

Figure 1. Schematic of the Ames Holographic Interferometer.

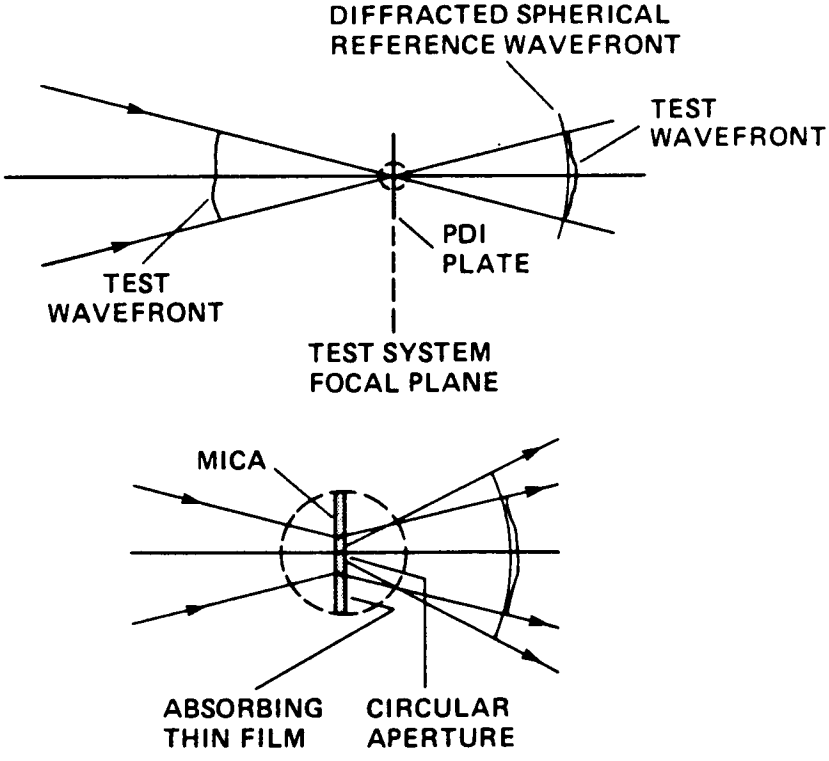

Figure 2. Schematic of the Smartt Point Diffraction Interferometer.

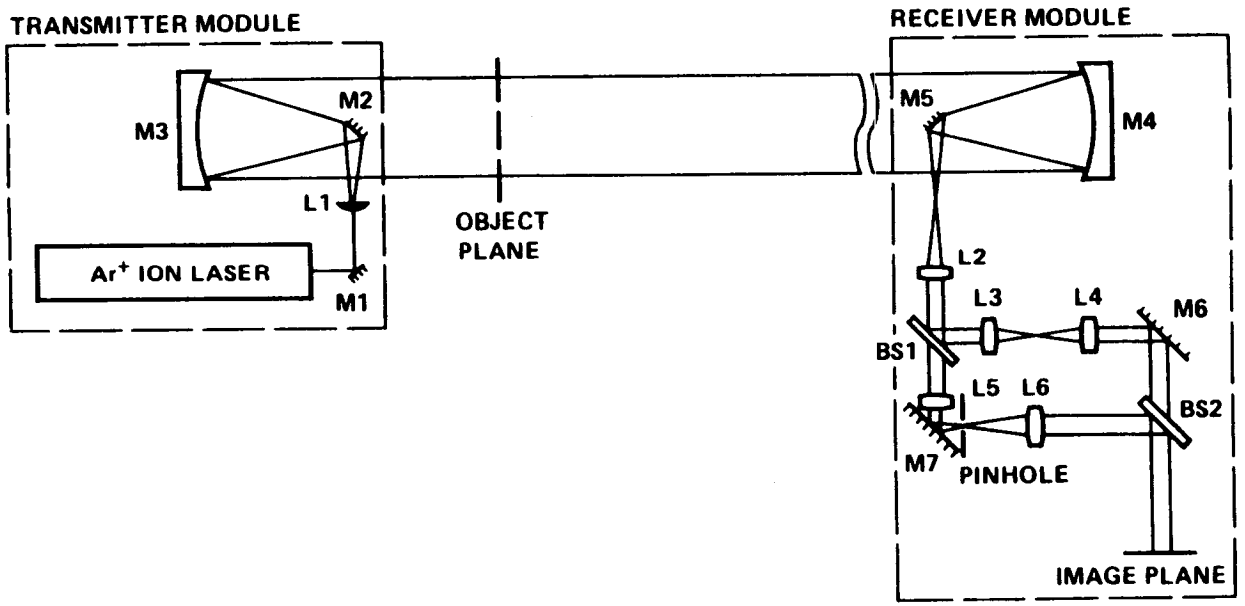

Figure 3. Schematic of the Improved Point Diffraction Interferometer.

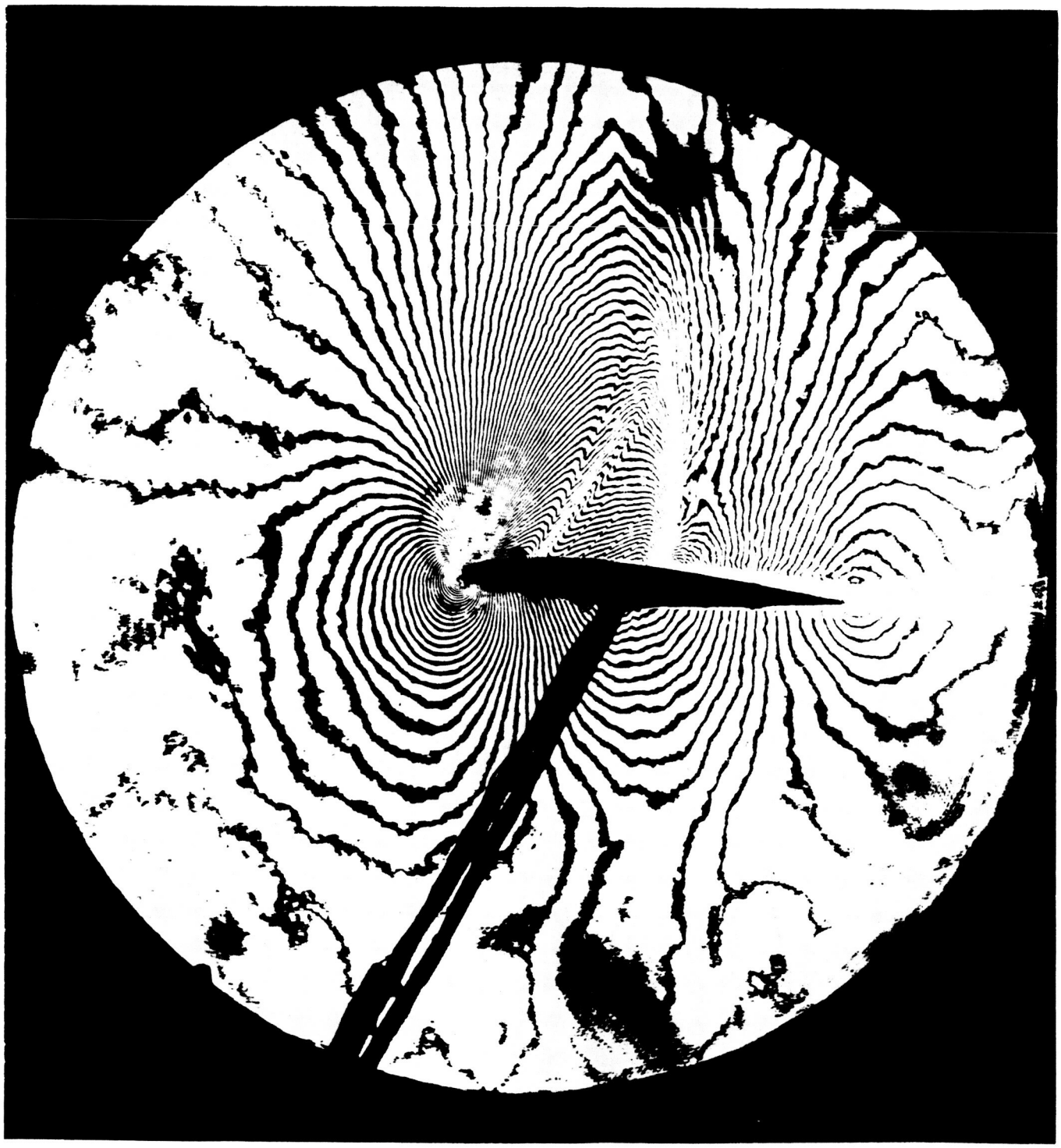

Figure 4. Infinite - Fringe Interferogram of NACA 64A010 at $M_{\infty} = 0.8$, $\alpha = 3.5^{\circ}$.

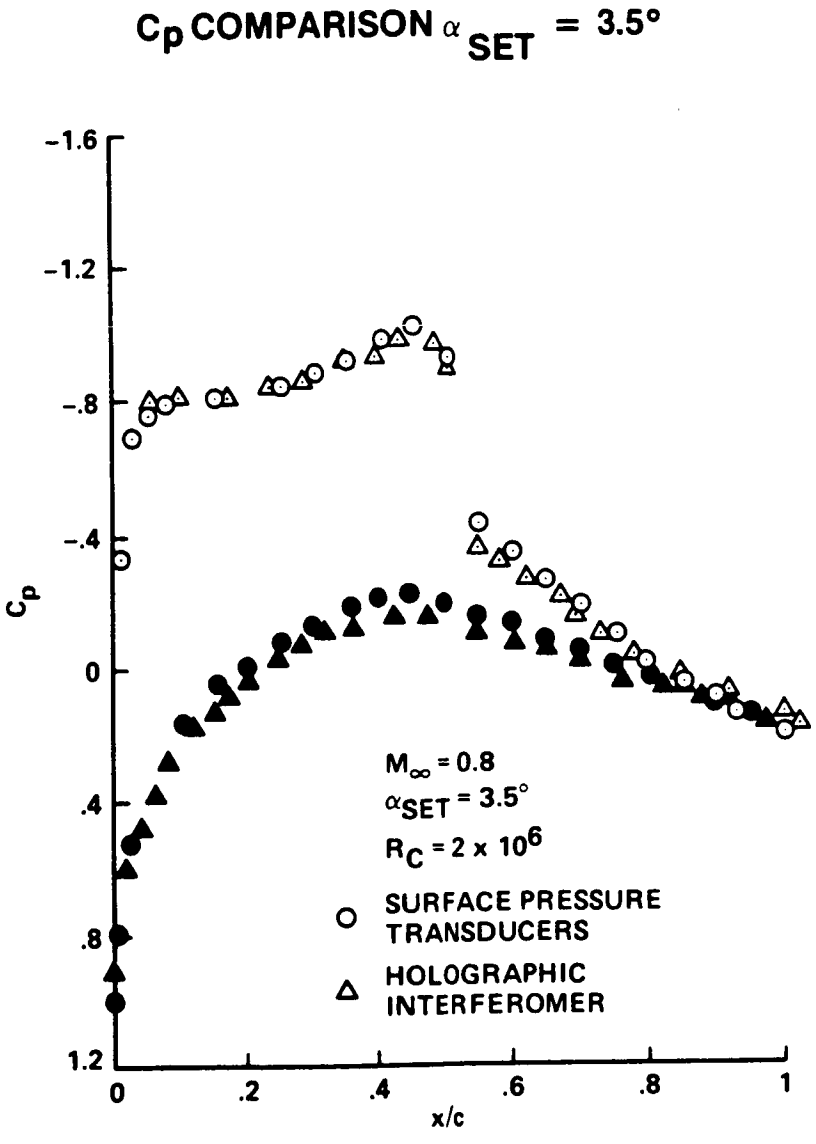

Figure 5. Comparison of Boundary-layer Edge pressures with Surface Pressure.

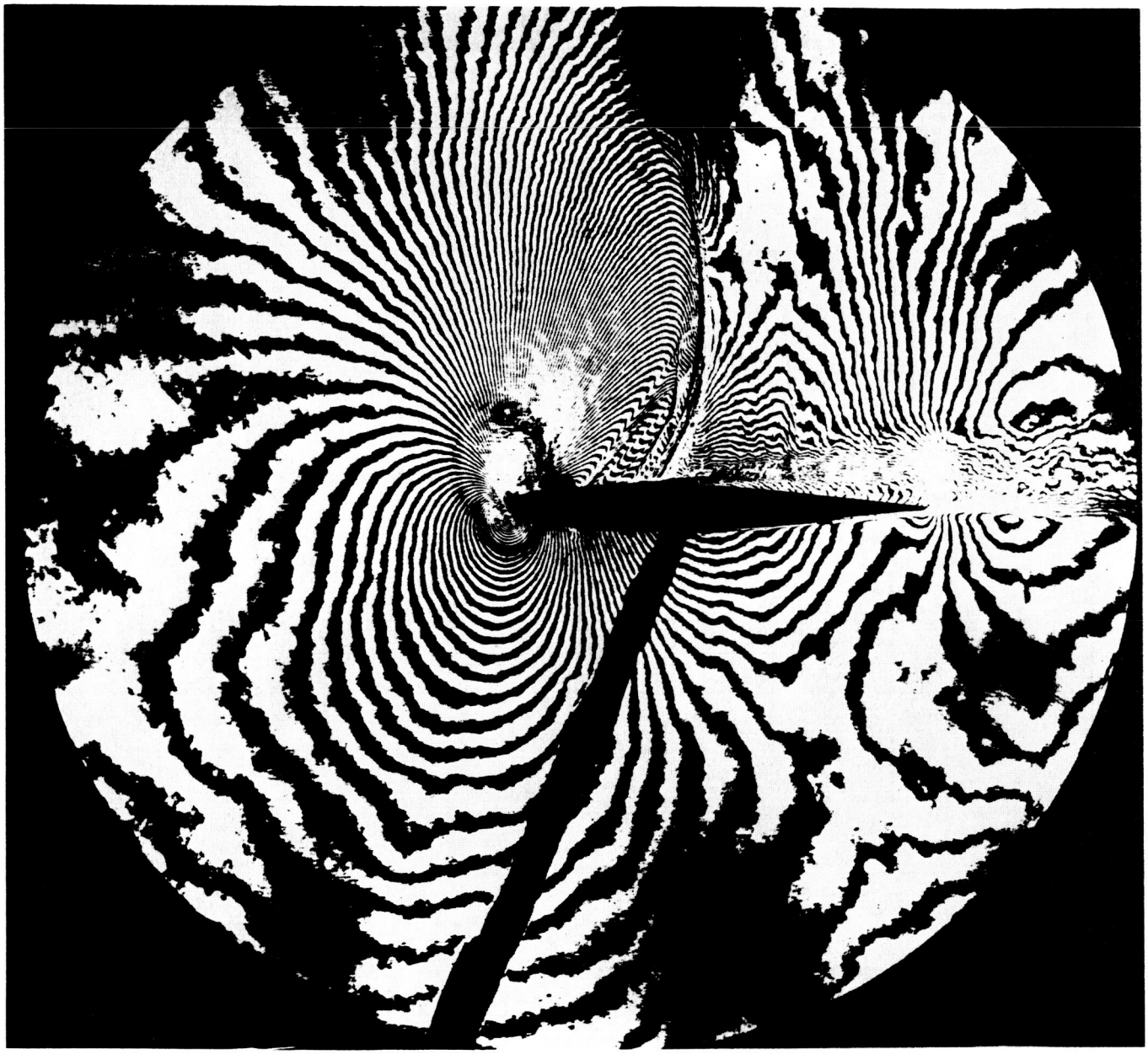

Figure 6. Infinite - Fringe Interferogram of NACA 64A010 at $M_\infty = 0.8$, $\alpha = 6.2^\circ$

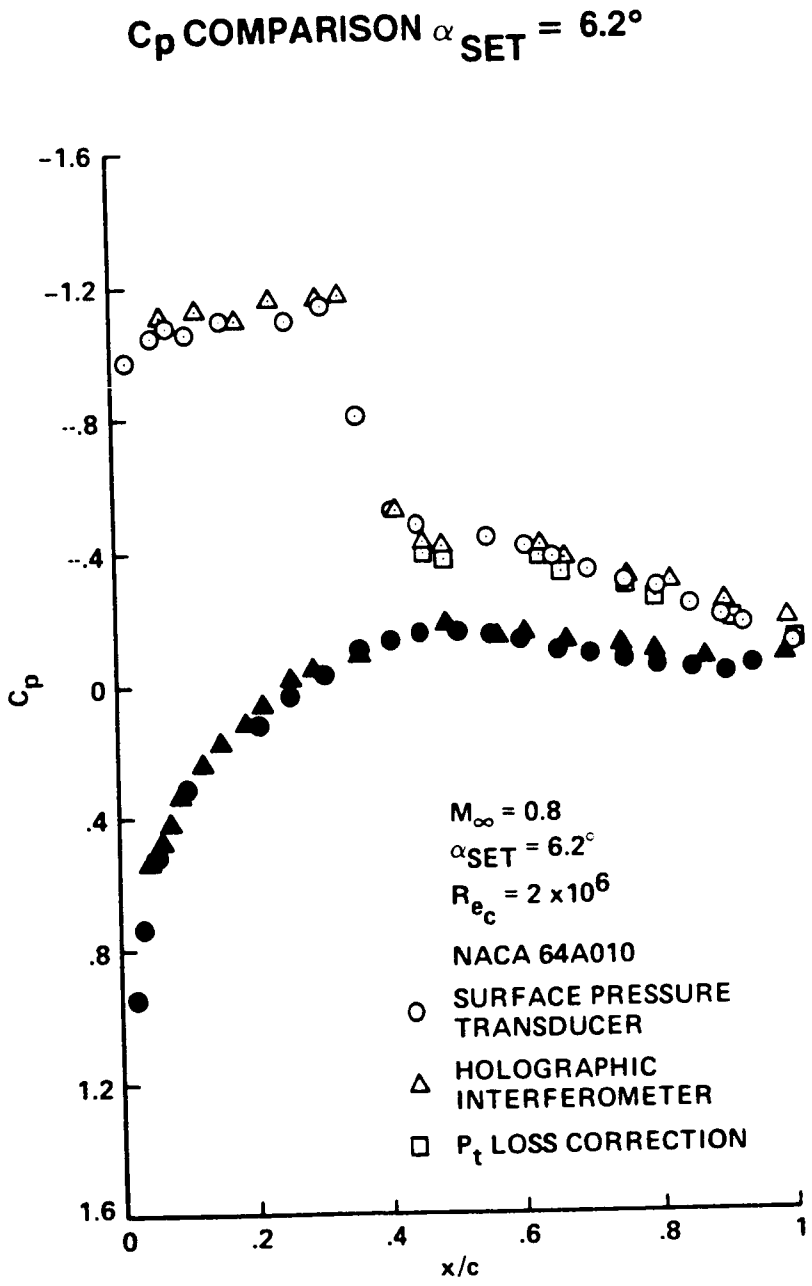

Figure 7. Comparisons of Measured Surface Pressure Coefficients.

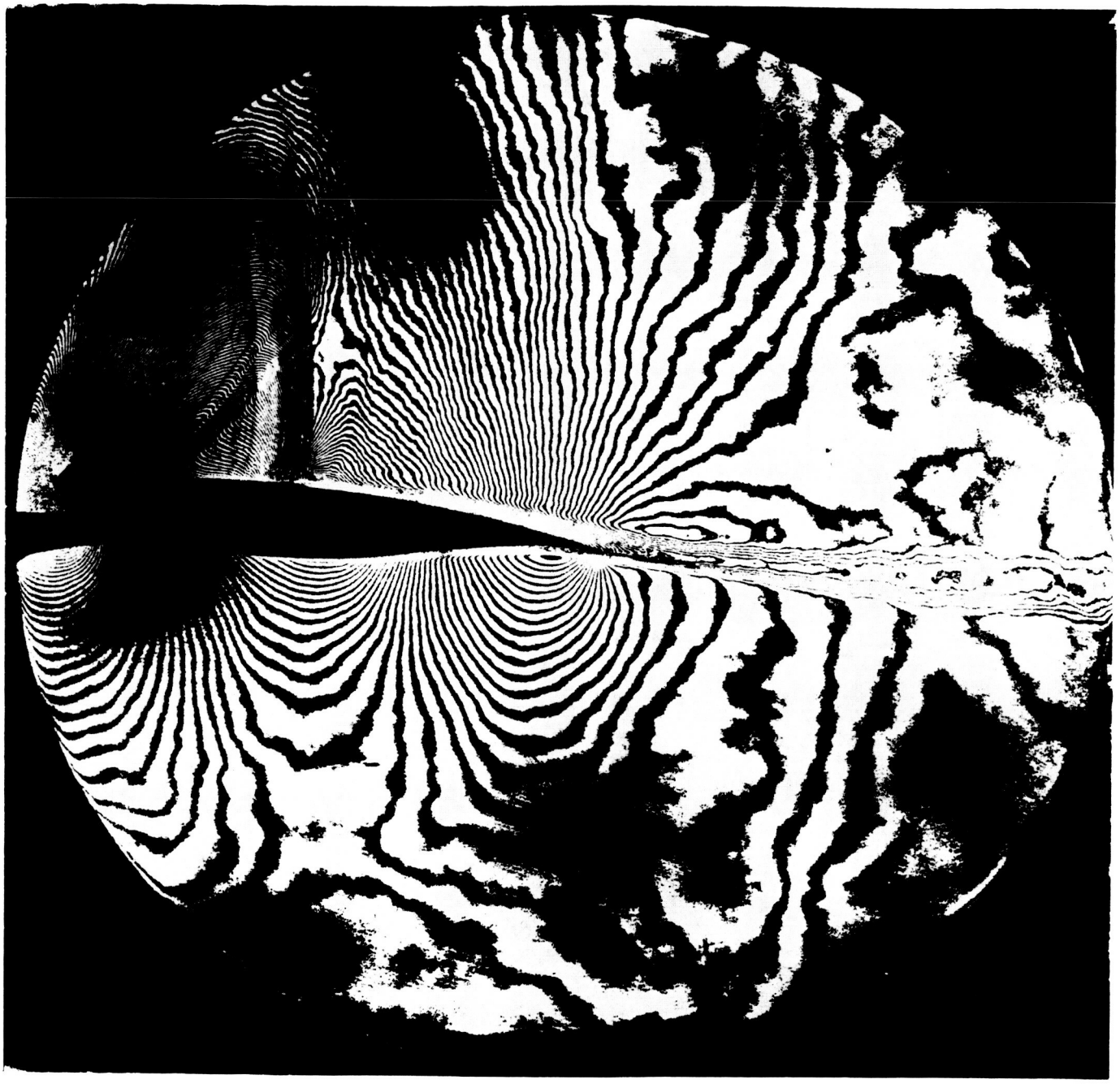

Figure 8. Interferograms of DSMA 671 Supercritical Airfoil Flow Fields, $M_\infty = 0.5$, $= 6.1^\circ$.

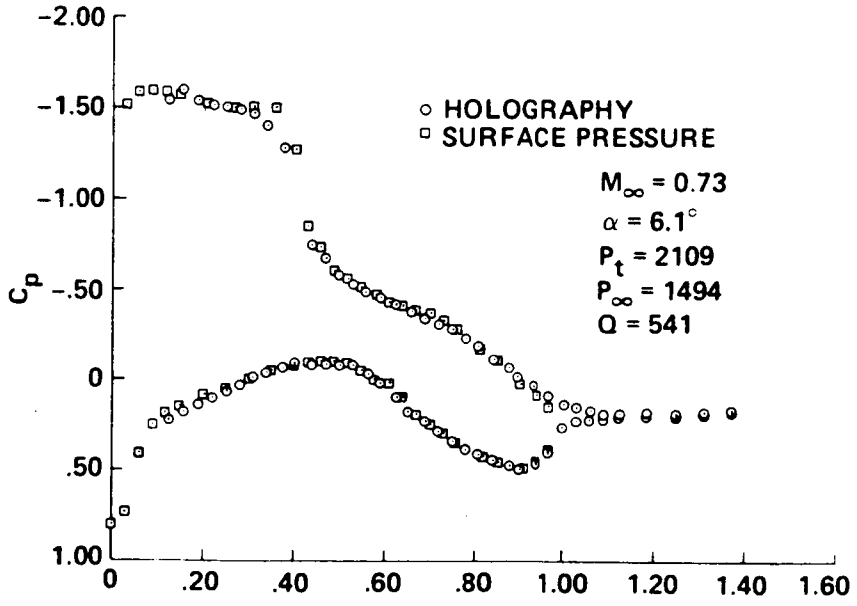

Figure 9. Comparisons of Data from Static Pressure Orifices and Pressures Determined from the Interferograms.

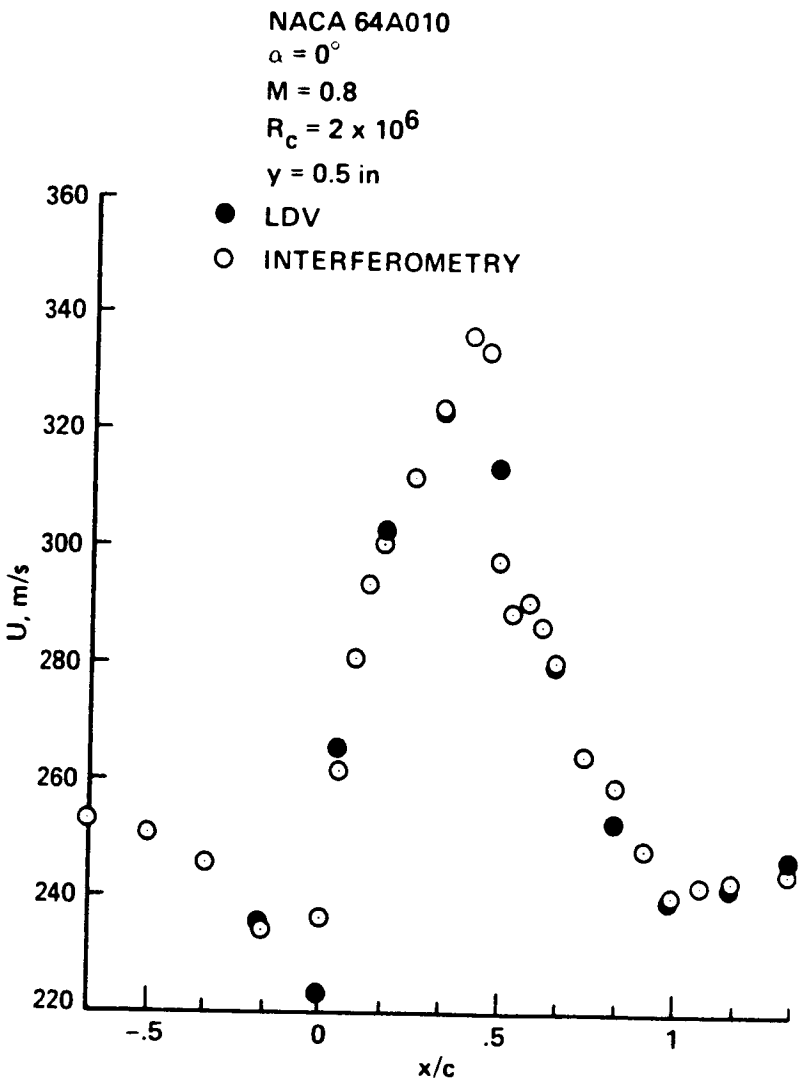

Figure 10. Flow Speed Distribution Measured with the Interferometer and the Laser Doppler Velocimeter.

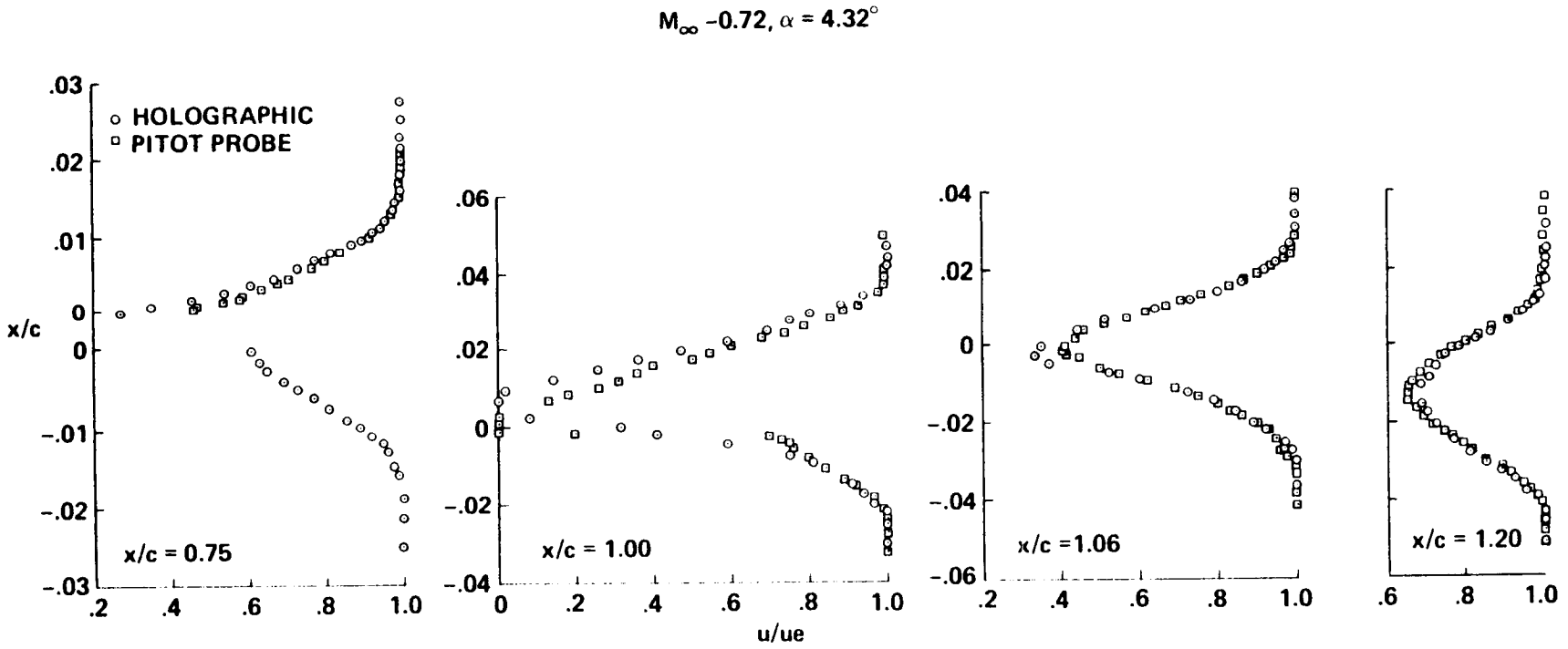

Figure 11. Trailing-edge Boundary Layer and Wake Profiles.

Figure 12. Interferogram of the Circulation Control Airfoil Flow.

13a. Coanda Jet Off.

Figure 13. Enlargements of the Trailing-edge Flow Fields.

13b. Coanda Jet On.

Holographic
Interferometry

Point Diffraction
Interferometry

Figure 14. Comparisons of Holographic and Point Diffraction Interferometry